行政院國家科學委員會專題研究計畫　期中進度報告

電注入連續性操作光子晶體雷射的製程開發與特性的設計和量測(1/2)

計畫類別： 個別型計畫
計畫編號： NSC93-2215-E-009-059-
執行期間： 93 年 08 月 01 日至 94 年 07 月 31 日
執行單位： 國立交通大學光電工程學系(所)

計畫主持人： 李柏璁

報告類型： 精簡報告
報告附件： 出席國際會議研究心得報告及發表論文
處理方式： 本計畫可公開查詢

中　華　民　國 94 年 5 月 31 日

行政院國家科學委員會補助專題研究計畫 **□ 成 果 報 告**
□期中進度報告

電注入連續性操作光子晶體雷射的製程開發與特性的設計和量測(1/2)

計畫類別： ☑ 個別型計畫　　□ 整合型計畫
計畫編號： NSC-93-2215-E-009-059
執行期間： 2004 年　08 月　01 日至 2005 年 07 月 31 日

計畫主持人：李柏璁 助理教授
計畫參與人員：盧贊文，趙紘鈞，張吉東，蔡豐懋

成果報告類型(依經費核定清單規定繳交)：精簡報告

本成果報告包括以下應繳交之附件：
□赴國外出差或研習心得報告一份
□赴大陸地區出差或研習心得報告一份
□出席國際學術會議心得報告及發表之論文各一份
□國際合作研究計畫國外研究報告書一份

處理方式：除產學合作研究計畫、提升產業技術及人才培育研究計畫、列管計畫及下列情形者外，得立即公開查詢
□涉及專利或其他智慧財產權，□一年□二年後可公開查詢

執行單位：

中　華　民　國　　年　　月　　日

（一）中文摘要

在這份報告我們呈現從 2004 年 8 月到 2005 年 5 月的研究成果。延續先前的研究，我們利用新的 ICP/RIE 製程方式製作光子晶體瑕疵共振腔，同時也成功的發展出 DBR bonding 的技術。我們也已經發展並自行撰寫出光子晶體主動元件的模擬系統，包括了關鍵性的二維及三維有限元素時域差分法（2D & 3D FDTD methods）用以分析光子晶體雷射激發模態以及光子晶體能帶圖。此外，我們將原有的長波長共焦顯微光譜系統優化至次奈米光譜解析度以及次微米顯微解析度，利用這套系統我們分析了對稱型光子晶體瑕疵共振腔的基本特性及各種熱效應，這一連串的分析對於 CW 操作的達成是極為重要的依據。

關鍵詞：光子晶體，半導體雷射，瑕疵共振腔，有限元素時域差分法模擬

（二）英文摘要

The research progress during the project period from August, 2004 to May, 2005 on photonic crystal laser cavities is presented in this report. The complete fabrication processes of photonic crystal micro-cavities using the new-purchased ICP/RIE equipment and DBR bonding technology have been developed. The lasing mode profiles and the photonic band structures are also calculated by 2D and 3D FDTD methods. In addition, the basic characteristics and thermal properties of photonic crystal micro-cavities have been measured and analyzed in details by using the optimized micro-PL system with sub-nano spectrum and microscopic resolutions.

Keywords: photonic crystals, semiconductor lasers, defect cavities, FDTD simulations

報告內容：

A. 研究方法：

1. 製程技術研發：
   (1). 利用新型的 ICP/RIE 製程，發展並製作光子晶體缺陷共振腔。
   (2). 基於舊有知識，發展新型 DBR bonding 技術。
2. 模擬系統建立及應用：
   (1). 利用 2D FDTD 模擬方法，模擬光子晶體缺陷共振腔雷射激發模態分佈。
   (2). 利用 3D FDTD 模擬方法，模擬光子晶體基本能帶圖。
3. 量測技術：
   (1). 優化長波長共焦顯微光譜系統。
   (2). 光子晶體雷射基本特性分析及各種熱效應分析。

B. 研究結果及討論：

I. Fabrication

Continue with our previous work, we present the complete fabrication process of two-dimensional photonic crystal micro-cavities in this report. In addition, DBR bonding technique for our future work is also developed based on our bonding technology developed during the last project period. Among our photonic crystal fabrication process steps, a new dry etching equipment, Inductively Coupled Plasma /Reactive Ion Etch (ICP/RIE) system, which was produced by Oxford Instruments Plasma Technology, is applied instead of the HDP dry etching step.

The membrane-type devices are fabricated in a dielectric material which consists of four compressively-strained InGaAsP MQWs separated by three unstrained InGaAsP barriers. It is confirmed that the PL spectrum is centered at 1550nm. The photonic crystal patterns are defined in the MQWs by a series of dry etching processes and a 220nm thickness membrane is formed by HCl wet etching.

At first, a 140nm-thickness SiNx layer is deposited on the InP cap layer by Plasma-Enhanced Chemical Vapor Deposition (PECVD) system with $SiH_4/NH_3/N_2$ gas. The photonic crystal patterns are defined by e-beam lithography on a 240nm polymer-thylmethacrylate (PMMA) layer. The procedure is described as follows：

1. Initial clean with Acetone and IPA
2. PMMA A-5 spin coating on SiN (coating mode D)
3. Soft bake at 180℃ for 90 seconds

4. E-beam lithography defining the photonic crystal patterns
5. Development with MIBK solution at 25~26℃ for 70 seconds
6. Fixing with IPA solution

An Oxford Instruments Plasma Technology Plasmalab system 100 ICP/RIE is used to transfer the PMMA patterns to SiNx layer and etch through the InGaAsP membrane layer into the InP substrate with SiNx layer as the hard mask. To maintain the integrity of the ICP/RIE chamber, O_2 plasma clean is periodically performed between each etching step. The ICP/RIE procedure is described as follows：

1. O_2 plasma for 3 seconds to remove the residual PMMA after the e-beam step
2. Etch SiNx (140nm) with the following condition：
   Reactive gas：CHF_3/O_2 = 50/5 sccm
   RF power = 150 W
   Chamber pressure fixed at 55mT, substrate temperature = 20℃
   Etching rate = 90nm/min, etch 105 seconds
3. O_2 plasma 20 seconds for removing the PMMA mask layer
4. O_2 plasma 90 seconds for the chamber cleaning (unload wafer)
5. Etch InGaAsP/InP (>300nm) with the following condition：
   Reactive gas：$H_2/CH_4/Cl_2$ = 19/23/14 sccm
   ICP power = 1000 W, RF power = 73 W
   Chamber pressure fixed at 4mT, substrate temperature = 150℃
   Etching rate = 330nm/min, etch 55seconds
6. Etch SiNx for removing the mask layer
   Reactive gas：CHF_3/O_2 = 50/5 sccm
   RF power = 150 W
   Chamber pressure fixed at 55mT, substrate temperature = 20℃
   Etching rate = 90nm/min, etch 60seconds
7. O_2 plasma 10 minutes for the chamber cleaning (unload wafer)

The SEM pictures of photonic crystal patterns on InP and GaAs substrates after dry etching process are shown in Fig. 1(a) and (b). The excellent hole profile and the vertical sidewall can be observed in these pictures.

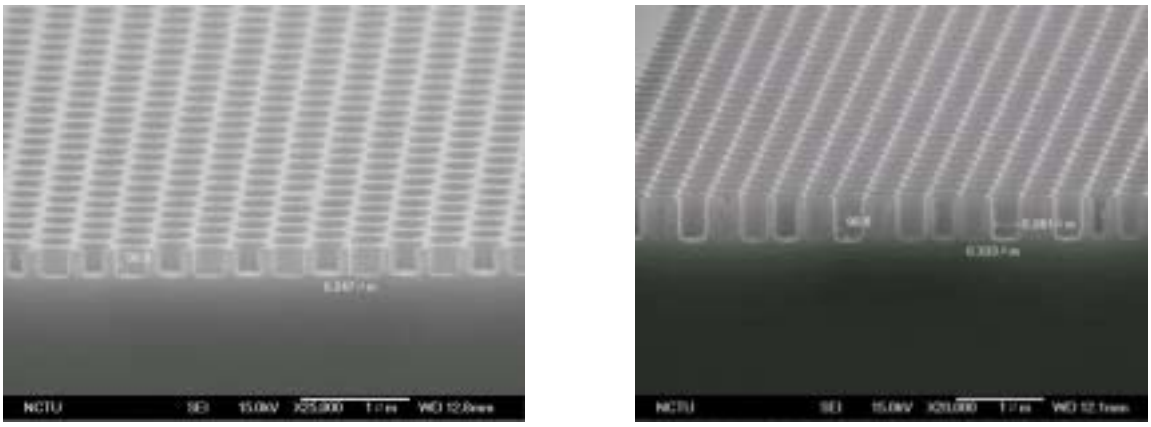

(a). (b).

Fig. 1. The SEM pictures of photonic crystal patterns on (a) InP and (b) GaAs substrates fabricated by ICP/RIE process.

At last, the membrane structure is formed by using a mixture of HCl and water. The HCl solution etches the InP layer at a faster rate than it does the InGaAsP active layer, providing the necessary degree of etch selectivity. This process also smoothes most of the sharp features on the sidewalls of the holes, which decreases the optical loss caused by the roughness. The wet etching is done at 0℃ where the resolution and selectivity of the etch are improved by cooling down the solution.

The consequence of this anisotropic etching is shown in Fig. 2(a) and (b). The HCl etching effectively stops at 93.6 and 32.9 degrees from the <-1,0,0> direction in the (0,-1,-1) plane and the (0,1,-1) plane, respectively. The membrane structure is formed by this wet etching process. The SEM picture of two-dimensional photonic crystal laser is shown in Fig. 2.

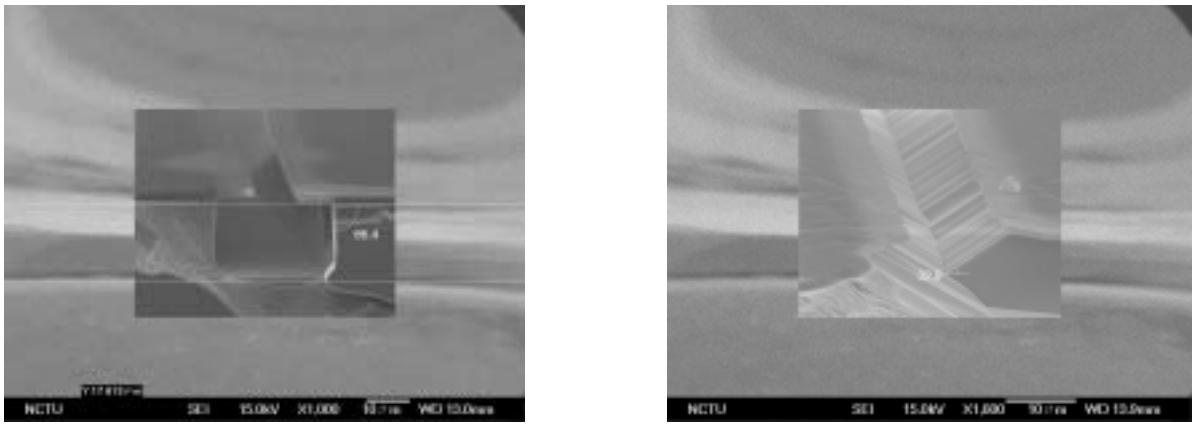

(a). (b).

Fig. 2. The etching stop planes of InP in (a) <-1,0,0> and (b) <0,-1,-1> directions.

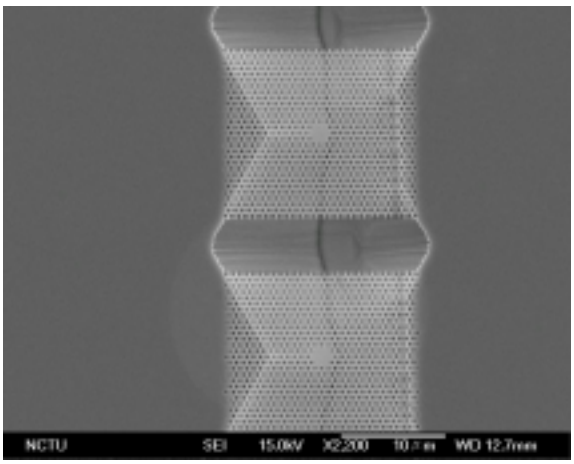

Fig. 3. The SEM pictures of two-dimensional photonic crystal micro-cavities.

Wafer-bonding technology is successfully developed in our previous researches. In order to reduce the optical loss caused by the asymmetric structure, DBR bonding is proposed and realized. We have developed this technology by using the similar methods in H_2 environment at 600°C and the DBR bonding sample is shown in Fig. 4. This would be the critical technology for our new devices.

Fig. 4. The DBR bonding sample.

II. Simulation

1. Improvements on FDTD simulation

To increase the efficiency of calculation, we rewrite the code of the program in C language under Linux operation system and PC with 64-bit CPU. It improves the computing speed greatly. For example, it takes around 1.3 seconds per loop without extra data process. It is more than 100 times faster than the elder version of the same problem. To save the memory required during the simulation, we change the data type of variable from "double" to "float". And we use the Heaviside-Lorentz unit system in order to get more numerical precision instead of typical MKS unit system.

The reflection of waves from the boundaries may cause redundant fields which we don't want inside

the simulation domain. To avoid this phenomenon, various absorbing boundary conditions (ABCs) were employed. In previous simulation, Mur's second order ABCs were used because it is easy for coding and needs less computing resource. However, it also brought some disadvantages. The numerical unstability comes after thousands of time steps as the simulation runs.

For this reason perfectly matched layer (PML) ABC is used instead of Mur's second order ABCs. The basic idea behind the PML scheme is the introduction of artificial conducting material that absorbs waves but does not reflect them. Although it costs more computing resource, it provides better efficiency for absorbing outgoing waves.

2. 2D FDTD simulation for mode profiles and quality factors

The following shows an example of finding the resonant frequency, mode profile, and quality factor of the monopole mode of the cavity. The calculated effective index of the fundamental TE mode of the slab is 2.65. The lattice constant is 0.525 μm. The defect is formed by removing single air hole from array of holes of hexagonal lattice arrangement. 5 layers of air holes surround the single defect. The six inner hole radii next to the defect are 0.1 μm, and the rest hole radii are 0.194 μm. The design of this structure is for wavelength around 1550nm.

The structure is shown in Fig. 5. Note that the structure is symmetry in both x- and y-directions (when z-direction is the direction out of the paper) so that we can apply symmetric boundary conditions at center of the structure. This helps us to reduce the size of the domain of simulation to one quarter of the original domain, thus the simulation time.

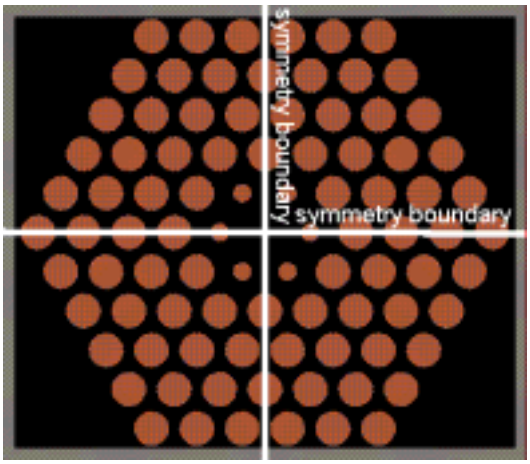

Fig. 5. The structure and the symmetric boundary condition.

Resonant frequencies of monopole mode are derived from frequency response at center position. It is excited by a short pulse of 10 femto-seconds with a broadband frequency covering the frequency of

interest. The pulse has only Hz component of TE mode. We found the peak frequency is located at 205 THz, so we run the simulation again with an excitation of point Gaussian source located in the center of the cavity of which central frequency is narrowly-peaked around the frequency of the desired mode (205 THz). Quality factor is also observed as 1130 from the slope of decay of the electromagnetic field amplitude. An example of mode profile of monopole mode in a single defect photonic crystal cavity is shown in Fig. 6.

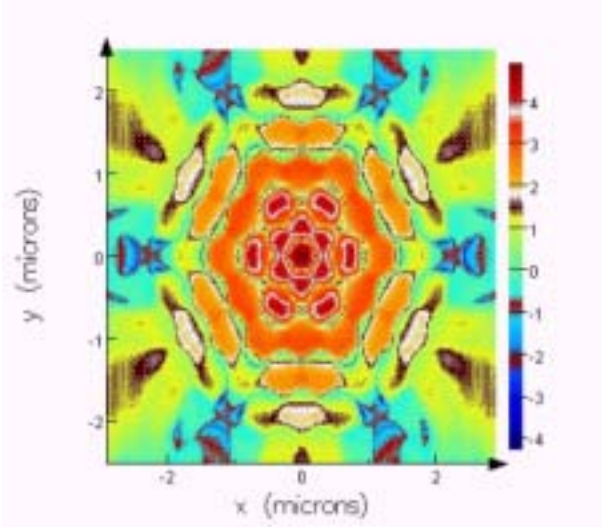

Fig. 6. The mode profile of monopole in log scale.

3. 3D FDTD simulation of bandstructure of 2D photonic crystal slab

We place magnetic dipole sources with short impulse of 3 femto-seconds at three different low symmetry positions of the unit cell. We record the time evolution of electromagnetic fields at another three low symmetry positions of the unit cell for more than 18000 time steps. The positions of dipole sources and monitors are shown in Fig. 7.

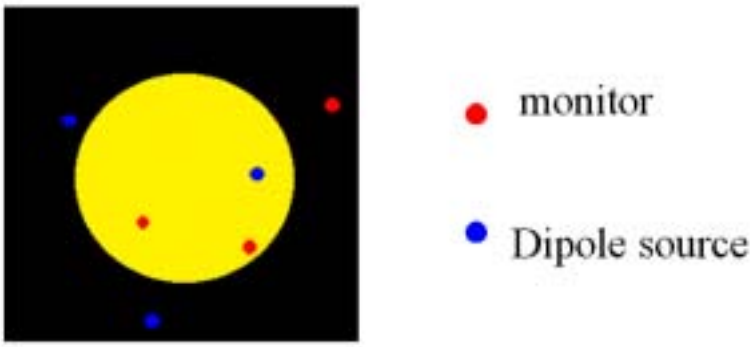

Fig. 7. The locations of sources and monitors.

Bloch's boundary conditions with specific wave vector are applied to the four sides of the unit cell.

PML ABCs are used in the directions outward and inward to this paper. To obtain the complete bandstructure we have to repeat the procedure for k-points along the first Brillioun zone in k-space. Then we collect three time signals and add them as a new signal. Normalize the signal with maximal amplitude. Apodize them using Gaussian function to exclude the undesired frequencies. Chirp z-transform the signal with a range of frequency of interest to observe the spectrum. Note that the missing points may result from the abandoning of small signals of 1/1000 smaller than the maximum peak. The bandstructure of a hexagonal lattice is shown in Fig. 8 as an example.

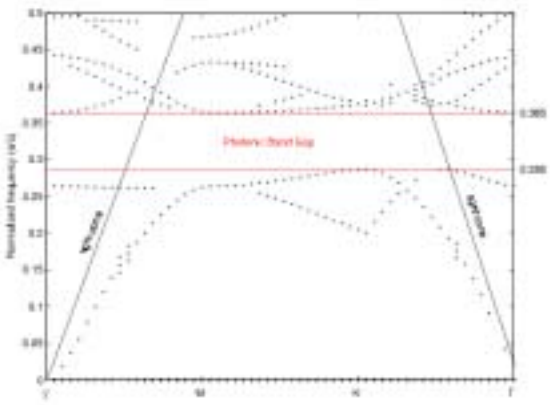

Fig. 8. The bandstructure of photonic crystal in hexagonal lattice.
(r/a = 0.3, d/a = 0.4, and n = 3.4)

III. Characterization and Thermal Analysis

In our previous work, the micro-PL system had been setup. Here we present the optimized system illustration with TTL laser pump source as shown in Fig. 9. Some basic characteristics of the photonic crystal micro-cavities can be measured using this system. In addition, the thermal characteristics have been analyzed in this section by using the TEC system we setup in our previous work.

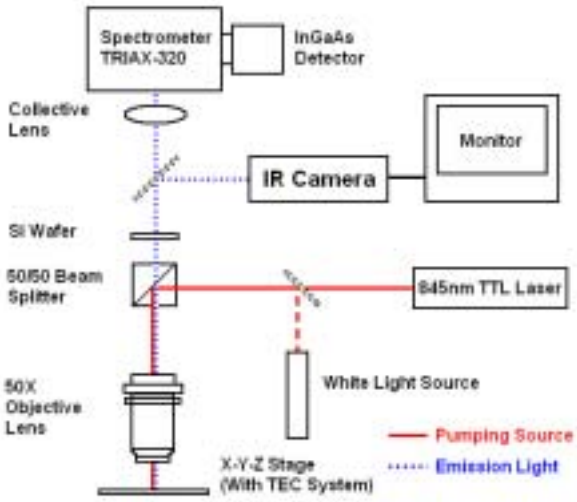

Fig. 9. The illustration of modified micro-PL system.

Our photonic crystal micro-cavity is formed by 19 missing air-holes as we mentioned before. A typical L-L curve of a photonic crystal laser with 500nm lattice constant and 0.25 r/a ratio is shown in Fig. 10. Its threshold can be estimated as 5.6μW. The lasing spectra near and above threshold are also shown in the insets of Fig. 9. The pump condition is 2% duty cycle with 0.5MHz repetition rate.

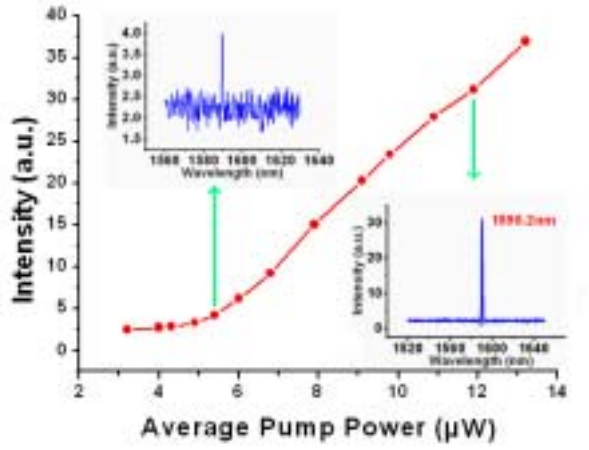

Fig. 10. L-L curve of a 2D photonic crystal laser pumped with 2% duty cycle at 0.5 MHz repetition rate. The insets are its lasing spectra near and above threshold.

In fact, there are a lot of resonance modes in this photonic crystal micro-cavity. We measure over ten resonance modes in this micro-cavity as shown in Fig. 11. Most of them are shown at wavelength from 1450nm to 1580nm due to their alignment with gain peak and the responsibility of our InGaAs detector. This can be good reference and modification guideline for our future work.

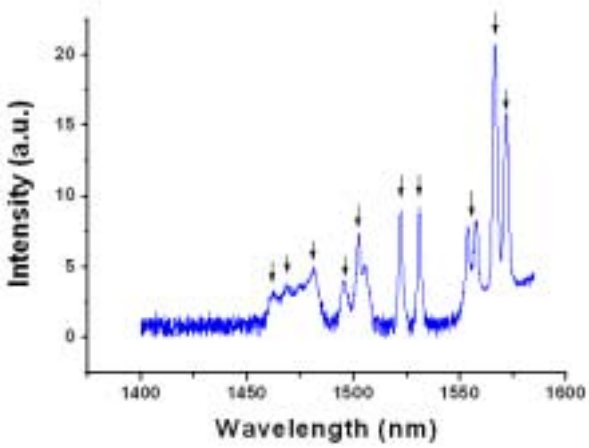

Fig. 11. Over ten resonance modes are observed in the photonic crystal D3 micro-cavity.

We also fabricate several photonic crystal laser arrays. In these arrays, we change their individual r/a ratio by varying their air-holes radius. The multi lasing spectra correspond to different components are shown in Fig. 12. This could be a very good application in the WDM communication systems.

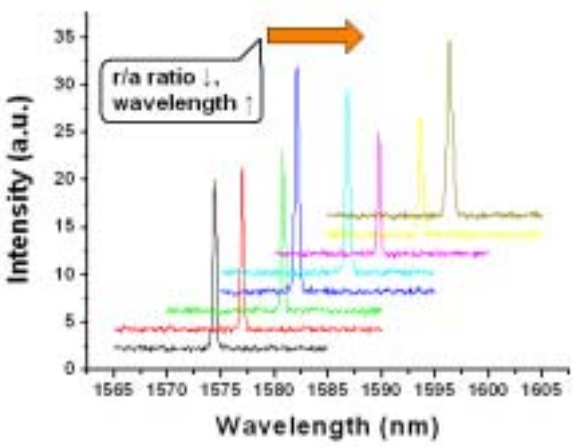

Fig. 12. Lasing wavelengths of photonic crystal laser arrays by changing their r/a ratio.

In order to optimize the design of sapphire-bonding photonic crystal lasers, we analyze the thermal characteristics of photonic crystal membrane lasers by using our TEC system. At first, we analyze its lasing wavelength variation with different substrate temperatures as shown in Fig. 13. Its lasing wavelength increasing rate is about 0.067nm/K. It matches quite well with the simulation result, 0.077nm/K, obtained by using FDTD methods. This thermal tuning property can also be an important application in WDM systems.

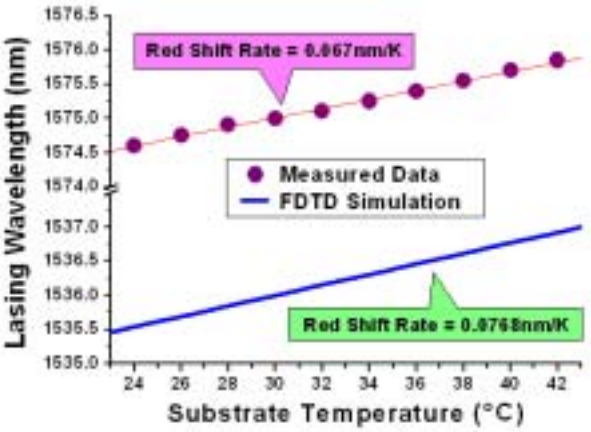

Fig. 13. Thermal tuning of lasing wavelength of a photonic crystal laser by changing the substrate temperature.

We also investigate the threshold dependence on different substrate temperatures and different pump duty cycles. The different thresholds correspond to different substrate temperatures and different pump duty cycles are shown in Table 1.(a) and (b).

Substrate Temperature	Threshold
24°C	6.8μW
30°C	10.3μW
36°C	14.8μW
42°C	20.2μW

(a).

Pump Duty Cycle	Threshold
1.0%	3.4μW
1.5%	4.3μW
2.0%	6.1μW

(b).

Table 1. (a). Threshold dependence on different substrate temperatures. (b). Threshold dependence on different pump duty cycles.

C. Publications：

[1] T.-W. Lu and P.-T. Lee, "**Thermal characteristics of two-dimensional photonic crystal lasers,**" *OPT'04*, B-SA-VII-1-6, Chun-Li, Taiwan (2004).

[2] T.-W. Lu and P.-T. Lee, "**Thermal characteristics of two-dimensional photonic crystal lasers,**" *IEEE WOCN'05*, 1064, Dubai, U.A.E. (2005).

[3] T.-W. Lu and P.-T. Lee, "**Thermal tuning and characterization of lasing properties of two-dimensional photonic crystal lasers,**" *submitted to Appl. Phys. Lett*. (2005).